Electromagnetic Signature of Prefracture Criticality in Heterogeneous Media

P. G. Kapiris,[1,*] K. A. Eftaxias,[1,†] and T. L. Chelidze[2]

[1]*Solid State Section, Physics Department, University of Athens, Athens, Greece*

[2]*Tbilisi State University, Tbilisi, Georgia*

(Received 21 January 2003; published 12 February 2004)

Fractal statistical analysis under the critical point (CP) hypothesis is applied to electromagnetic (EM) signals emitted before failure. A new approach to the analysis of a possible EM fractal pattern evolution toward CP is suggested. The analysis reveals characteristic signs of approaching the CP: the emergence of memory effects; the increase of the spatial correlation; the decrease of the antipersistence behavior; the appearance of persistence properties in the tail of the precursors, a loss of multifractality, and, finally, the divergence of the energy release rate. These critical features are compatible with the percolation theory of fracture process.

DOI: 10.1103/PhysRevLett.92.065702 PACS numbers: 64.60.Ht, 62.20.Mk, 64.60.Ak, 91.30.Px

When a heterogeneous material is strained, its evolution toward breaking is characterized by the nucleation and coalescence of microcracks before the final breakup. Both acoustic as well as EM emission in a wide frequency spectrum ranging from very low frequencies (VLF) to very high frequencies (VHF), is produced by microcracks, which can be considered as the so-called precursors of general fracture.

Field experimental results on EM emission associated with earthquakes (EQ) and interpretation in the framework of CP concept [1] are presented.

We consider the VLF (3 and 10 kHz), and VHF (41 and 54 MHz) EM emission patterns before the $M = 6.6$ Kozani-Grevena earthquake (K-G EQ) (13 May 1995, Greece) [2–4]. VHF signals of gradually increasing activity are clearly detectable and are of sufficiently long duration, i.e., $\sim$ several h (the data were sampled at 1 Hz), to provide adequate sample data for statistical analysis. At the tail of the VHF emission strong multipeaked EM signals of duration $\sim$30 min are detected. An almost simultaneous cessation of EM emission at both the kHz and MHz frequency bands was observed $\sim$1 h prior to the time of the earthquake (details on equipment and data processing are provided in Refs. [2,3]).

One feature that distinguishes the dynamics in a heterogeneous medium close to its final failure lies in the appearance of memory effects [5]. If the time series of amplitudes of the EM emission $A(t_i)$ is a temporal fractal then a power law spectrum density of the recorded time series is expected:

$$S(f) = \alpha f^{-\beta}. \quad (1)$$

The spectral amplification α quantifies the power of the spectral components. The linear correlation coefficient r is a measure of the quality of fit to the power law (1). A continuous wavelet transform (CWT) was used for the decomposition of our transient, nonstationary signals.

To show that we are near a critical transition we calculate the characteristic parameters α, β, r associated with successive intervals of 1024 measurements each and study the time evolution of these parameters.

The results presented in Fig. 1(a) exhibit a gradual increase of the correlation coefficient r with time as failure approaches. A region with r close to 1 is approached during the last few hours of the prefailure emission [second period on Fig. 1(a). Also, the number of time intervals with $r > 0.94$ increases progressively as the main shock approaches. The power law behavior described above breaks down just after the cessation of the VHF EM activity $\sim$1 h before the failure [third period on Fig. 1(a)].

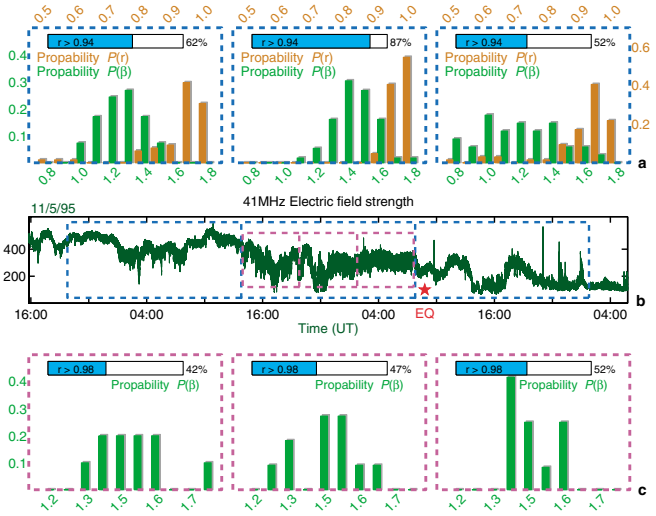

FIG. 1 (color). (a) Histograms of probability distribution of the correlation coefficient r and exponent β calculated on 1024 measurements segments for three consecutive time intervals (blue frames) marked in (b). Insets show the percentage of segments with $r > 0.94$. (b) The time series of the 41 MHz field strength [4]. The star indicates the time of the earthquake occurrence. (c) The probability distribution of the exponent β and the percentage of segments with $r > 0.98$ for 3 consecutive subintervals (purple frames) of 6 h duration each as marked in (b).

The β value reveals a fluctuating behavior. Its variation with time decreases in the narrow range around the most probable value $\beta = 1.5$ at the terminal phase of the precursory phenomenon. This fluctuating behavior also breaks down after the cessation of the signal, after which the scatter of the β values increases significantly. The distribution of β exponents is shifted to higher values during the anomalous EM emission [second period on Fig. 1(a)]. The VHF time series during the second period has been divided into three subintervals in Fig. 1(b). It is evident that the closer the final stage of seismic process, the larger the percentage of segments with $r > 0.98$, and the larger the shift of β to higher values. This signifies an increase in spatial correlation during period 2.

Since we expect the prefailure EM signals to exceed the background noise just before the main event, we constructed a fence of intervals with $r > 0.98$ and $\beta = 1.5 \pm 0.2$. A progressive increase of the number of intervals with the previously mentioned representative β values is observed as the shock approaches [Fig. 2(a)]. This evolution breaks down just after the cessation of the EM anomaly, $\sim$1 h prior to the event. The observed scaling law corroborates the presence of memory in the underlying fractoelectromagnetic process.

Following Ivanov *et al.* [6], we examined multifractal properties of the VHF time series, namely, the spectrum of the fractal dimension $D(h)$ as a candidate precursor of the main shock (Fig. 3). Our analysis reveals that the ranges of local Hurst exponents ($0 < h < 0.2$ and $0.19 < h < 0.24$) with nonzero fractal dimension $D(h)$ indicate that the EM fluctuations exhibit anticorrelated behavior. Figure 3 also shows that as the CP approaches, the EM time series manifest: a significant loss of multifractal complexity, displaying a smaller range of values of h, and their fluctuations become less anticorrelated, as the dominant local Hurst h is shifted to higher value.

In this paragraph we argue that the VHF precursor is strongly influenced by heterogeneity that gives rise to antipersistent behavior, as the areas with a low threshold for breaking alternate with much stronger volumes, where the crack growth stops (Fig. 3). The observed shift of local h exponents toward greater values can be understood if we accept that the microheterogeneity of the system becomes less anticorrelated with time.

Our conclusion appears to contradict a well-known result on the transition from mono to multifractal behavior in the percolation model of breakdown [7] at the last stage of the fracture process. The contradiction can be explained by a difference in the approach to the final stage of fracture. In simple percolation breakdown models the locations of new damaged sites stay random and noncorrelated even during the last stages of fracture. In reality, the damage process is anisotropically correlated, which means that the probability of damage is larger near an existing defect and in the direction of the largest tensile strain [8]. Furthermore, the dynamical stage of rupture may begin earlier than the formation of an infinite cluster of cracks, spanning the whole system, i.e., when the critical Griffith's size cluster of defects appears in the material [9]. Both these factors undoubtedly diminish the fractal dimension of the network of microcracks during the last stages of fracture. This explains the difference between our results and de Arcangelis and Herrmann [7] model.

We now focus on the VLF signal [Fig. 4(a)], detected at the tail of the VHF signal, i.e., just before the final quiescence preceding the main shock. This is a reasonable behavior if one accepts that cracks interact and coalesce to form larger cracks (as the failure approaches) and larger source dimensions are associated with the increase in the low frequency content of the emitted waves. This behavior is also in agreement with the observed shift (from MHz to kHz) of the acoustic activity during the prefailure stage (90–100% of the failure strength) [10]. The power spectrum density of the VLF activity also exhibits a decreasing power law behavior $S(f) \sim f^{-\beta}$ with two different branches, one at the lower $r = 0.92$,

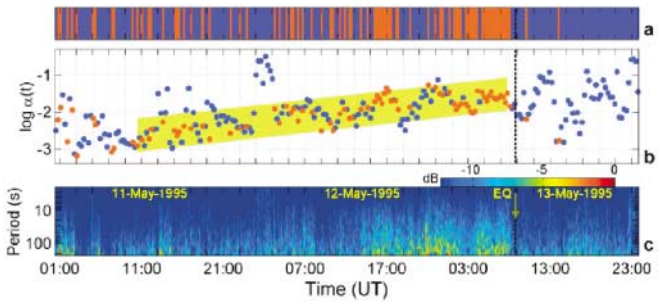

FIG. 2 (color). (a) The β values are confined in the narrow range $\beta = 1.5 \pm 0.2$ during the last few hours of the prefailure period while the fit to the power law model remains excellent ($r > 0.98$) for the whole extent of this period (see text). In the fence, the red stripes refer to 1024 measurements segments with ($1.3 < \beta < 1.7$ and $r > 0.98$). A progressive increase of the time intervals showing these characteristics as the failure approaches is observed. (b) The temporal evolution of the spectral amplification α corresponding to segments with $r > 0.98$, reveals a nearly exponential increase during the last several hours prior to the main event. The red circles correspond to segments with $r > 0.98$. (c) The wavelet power spectrum of the 41MHz EM time series.

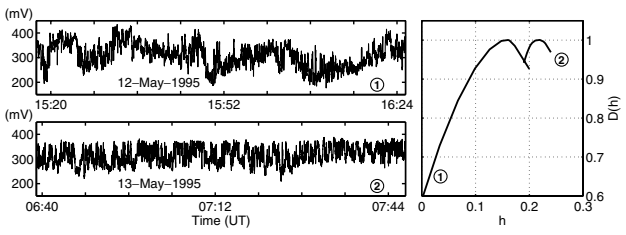

FIG. 3. Two segments of the precursory 41 MHz EM signal, recorded on 12 May 1995 (upper row) and 13 May 1995 (lower row). On the right part of the figure the corresponding fractal dimensions $D(h)$ are presented.

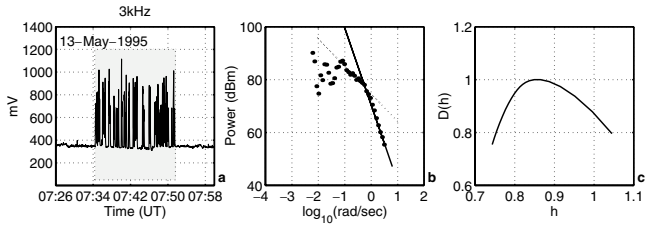

FIG. 4. (a) The 3 kHz EM emission before the K-G EQ [4]. (b) The power spectral density of the signal versus frequency. The straight lines reveal that the lower and higher frequencies follow a power law model with exponent β taking values 1.04 and 2.91, respectively. (c) The fractal dimension $D(h)$ at small scales, which correspond to higher frequencies.

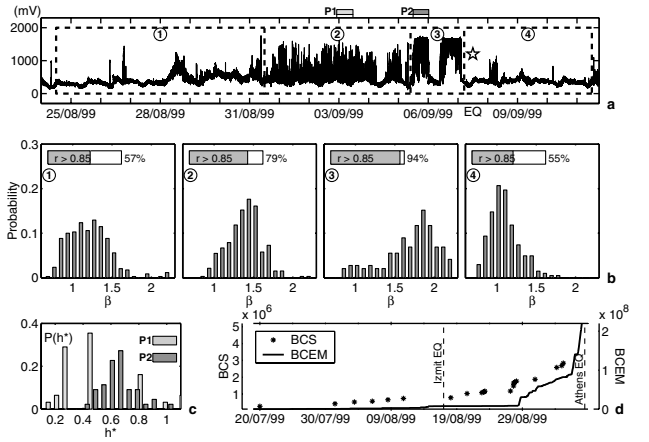

FIG. 5. (a) The time series of the 10 kHz magnetic field variations [4]. The star indicates the time of the Athens EQ occurrence. (b) Histograms of probability distribution of the exponent β calculated on 1024 measurements segments for four consecutive time intervals as marked in (a). Insets show the percentage of segments with $r > 0.85$. (c) The distributions of the statistically dominant local Hurst exponents h^* (see text) for two time periods (P1), (P2) noted in (b). (d) The evolution of Benioff cumulative strain release (BCS) and the Benioff cumulative EM energy release (BCEM) (see text). Provenance of seismicity data is http://www.gein.noa.gr/services/cat.html

$\beta = 1.04 \pm 0.03$ and another at the higher frequencies $r = 0.99$, $\beta = 2.91 \pm 0.03$ [Fig. 4(b)]. The power law at higher frequencies may reflect the dynamics within the bursts while the one at lower frequencies may indicate the correlation between the bursts. The multifractal analysis of this signal at small scales reveals that the EM fluctuations within the burst exhibit correlated behavior (local Hurst exponents centered at $h \approx 0.85$). This evidence may be regarded as a fingerprint of local dynamic rupture of asperities in the zone associated with the nucleation of the main rupture. Indeed, for times close to breakthrough, homogeneous backbones of high strength sustain the elastic strain energy. In the limit of a homogeneous system, once a crack nucleates in the rock, the stress is enhanced at its tip and therefore the next microcrack almost surely develops at the tip. The decrease of heterogeneity of the system appears to lead to a decrease in the ability to drive the system away from a persistence mode of cracking evolution. Hence, one does see long-range positive correlations in the associated part of the recorded time series. This might be an additional indication of emergence of a new phase in the development of criticality.

Now we consider the VLF EM signals associated with the Athens EQ ($M = 5.9$, 7 September 1999) [3,11] (Fig. 5). The whole long duration EM precursor [Fig. 5(a)] is characterized by an accelerating emission rate. This activity ends in two clear signals with an energy ratio (second to first signal) $\sim$5, and the radar interferometry analysis showed activation of two separate faults with corresponding energy release ratio (second to first) of 5 [11]. This surprising correlation in the energy domain hints a causal connection between the two events. This hypothesis is reinforced by the fractal analysis of the EM-time series. Indeed, one can recognize that the closer the final stage of seismic process, the larger the percentage of segments with $r > 0.85$, and the larger the shift of β to higher values [Fig. 5(b)]. We have calculated the fractal dimension spectrum $D(h)$ associated with successive intervals of 1024 measurements each, for two time periods P1, P2 [Fig. 5(a)]. In each interval the h^* represents the statistically dominant local Hurst exponent, i.e., the $D(h^*) \approx 1$ [6]. Figure 5(c) shows the distributions of h^* values for the above mentioned time periods. A transition from antipersistence to persistence is observed as the most probable h^* shifts to h values greater than 0.5. This matter agrees with laboratory experiments [12]. The pulselike morphology of the VLF signal with abrupt start and finish may also point to the persistent mode of the process at this stage, when due to the high level of clustering of defects, even a small crack, if it connects large clusters, may generate a large event [9].

The surface trace of a single major fault has a fractal dimension $D \approx 1.2$, whereas at small and lab scales $D \approx 1.6$–1.7 [13]. The number of bonds that break scales as $L^{1.7}$ with the system size L [14]. An opening crack, due to emitting, diffusing, and recombination charge, can act as an EM emitter. Fractal electrodynamics [15] suggests that the radiation from a fractal structure has fractal dimension equal to that of the emitting channel [16]. As we mentioned earlier, at the final stage the crack network can became less ramified. The features mentioned justify the observed evolution of the β values with time, and the difference between the β values associated with the first stage of the Athens EM precursory VLF time series and the β values corresponding to the VLF EM emission recorded prior to the K-G EQ; the difference may be associated with fractal patterns of fault network.

It is worth mentioning that both K-G and Athens EQs occurred right after the maximum of the variation of the β exponent. This is a reasonable behavior if we accept

that the observed increase of the correlation length in the EM-time series signalizes corresponding increase of the spatial correlation length in the preparation volume as the CP approaches.

A basic hallmark of the CP concept is the divergence of the rate of energy dissipation near the main event [1]. We investigate this feature from the EM point of view. First we focus on the K-G EQ. The wavelet power spectrum indicates a progressive increase in the amplitude of the VHF precursory events and a higher emission rate [Fig. 2(c)]. Spectral analysis confirms the presence of an accelerating emission rate in the prefailure activity. The temporal evolution of the spectral amplification α, corresponding to segments with $r > 0.98$, reveals a nearly exponential increase during the last several hours prior to the main event [Fig. 2(b)], implying that the heterogeneous system approaches criticality. In the case of the Athens EQ, acceleration of EM energy release was also observed [Fig. 5(d)]. The wavelet power spectrum also indicates a progressive increase in the amplitude of the VLF precursory events and a higher emission rate [11]. Moreover, the Benioff cumulative strain release $\varepsilon(t)$, computed over circle $R = 110$ km at the epicenter of the Athens EQ as a function of time along with the "Benioff" cumulative EM energy release exceeding a threshold (in arbitrary units) is depicted in Fig. 5(d), where $\varepsilon(t) = \sum_{i=1}^{N(t)} E_i(t)^{1/2}$ where E_i is the energy released by the ith EQ. We draw attention to the similarity of the temporal evolution of both the mechanical and the EM energy release as the main event approaches. The accelerated energy release in the final stages of fracture process is predicted in the percolation model of transitional amplitudes, suggested in [8,17] and numerical simulations [18].

Finally, the reported period of EM quiescence just before the EQ, observed both in the field and laboratory experiments, can be explained in terms of a catastrophic decrease in the elastic modulus M close to mechanical percolation threshold: $M \sim |x - x_c|^f$, where $f \sim 3.6$ for 3D systems [19]. The sudden drop of M means that the amount of elastic energy that can be released during crack nucleation (merging) decreases abruptly at $x \rightarrow x_c$; consequently, the amplitudes of acoustic and EM emissions may decrease before final rupture [20].

Modeling of mechanical and electrical properties of rocks near the percolation threshold [21] seem to explain critical behavior of the prefailure EM signals detected at various frequency bands from ULF up to VHF.

In summary, a new method to assess the approach to the CP (failure) is suggested, namely, the monitoring of evolution of several fractal characteristics of EM emission toward criticality in consecutive time windows. As the main event approaches, the number of intervals with fractal characteristics close to critical values increases significantly. The evolution of fractal patterns of EM emissions observed is in accordance with the CP hypothesis [1] and the percolation theory of fracture.

*Electronic address: pkapiris@cc.uoa.gr
†Electronic address: ceftax@phys.uoa.gr

[1] D. Sornette and C. G. Sammis, J. Phys. I (France) **5**, 607 (1995); H. Saleur, C. G. Sammis, and D. Sornette, J. Geophys. Res. **101**, 17 661 (1996);C. G. Sammis and D. Sornette, Proc. Natl. Acad. Sci. U.S.A. **99**, 2501 (2002); J. C. Anifrani, C. Le Floc'h, D. Sornette, and B. Souillard, J. Phys. I (France) **5**, 631 (1995).
[2] K. Eftaxias, P. Kapiris, E. Dologlou, J. Kopanas, N. Bogris, G. Antonopoulos, A. Peratzakis, and V. Hadjicontis, Geophys. Res. Lett. **29**, 69/1 (2002); P. Kapiris, J. Polygiannakis, A. Peratzakis, K. Nomikos, and K. K. Eftaxias, Earth Planets Space **54**, 1237 (2002).
[3] K. Eftaxias, P. Kapiris, J. Polygiannakis, A. Peratzakis, J. Kopanas, G. Antonopoulos, and D. Rigas, Nat. Hazards Earth Syst. Sci. **3**, 217 (2003).
[4] See EPAPS Document No. E-PRLTAO-92-044404 for the datasets. A direct link to this document may be found in the online article's HTML reference section. The document may also be reached via the EPAPS homepage (http://www.aip.org/pubservs/ epaps.html) or from ftp.aip.org in the directory /epaps/. See the EPAPS homepage for more information.
[5] H. Stanley, Rev. Mod. Phys. **71**, S358 (1999).
[6] P. Ivanov, L. N. Amaral, A. Goldberger, S. Havlin, M. Rosenblum, Z. Struzic, and H. Stanley, Nature (London) **399**, 461 (1999).
[7] L. de Arcangelis and H. J. Herrmann, Phys. Rev. B **39**, 2678 (1989).
[8] Y. Kolesnikov and T. Chelidze, J. Phys. A **18**, L273 (1985).
[9] T. Chelidze, Pure Appl. Geophys. **124**, 731 (1986).
[10] M. Ohnaka and K. Mogi, J. Geophys. Res. **87**, 3873 (1982).
[11] K. Eftaxias, P. Kapiris, J. Polygiannakis, N. Bogris, J. Kopanas, G. Antonopoulos, A. Peratzakis, and V. Hadjicontis, Geophys. Res. Lett. **28**, 3321 (2001).
[12] A. Ponomarev, A. Zavyalov, V. Smirnov, and D. Lockner, Tectonophysics **277**, 55 (1997).
[13] M. Sahimi, M. Robertson, and C. Sammis, Phys. Rev. Lett. **70**, 2186 (1993); A. Sornette, P. Davy, and D. Sornette, Phys. Rev. Lett. **65**, 2266 (1990).
[14] L. de Arcangelis, A. Hansen, H. J. Herrmann, and S. Roux, Phys. Rev. B **40**, 877 (1989).
[15] D. Jaggard, in *Recent Advances in Electromagnetic Theory*, edited by H. Kritikos and D. Jaggard (Springer-Verlag, Berlin, 1990), pp. 183.
[16] G. Vecchi, D. Labate, and F. Canavero, Radio Sci. **29**, 691 (1994); D. H. Werner and P. L. Werner, Radio Sci. **30**, 29 (1995).
[17] T. Chelidze and Y. Kolesnikov, J. Phys. A **17**, L791 (1984).
[18] M. Xia, Y. Wei, F. Ke, and Y. Bai, Pure Appl. Geophys. **159**, 2491 (2002).
[19] M. Sahimi and J. Goddard, Phys. Rev. B **33**, 7848 (1986).
[20] T. Chelidze, Terra Nova **5**, 421 (1993).
[21] D. Sornette, M. Lagier, S. Roux, and A. Hansen, J. Phys. (France) **50**, 2201 (1989); G. Gaillard-Groleas, M. Lagier, and D. Sornette, Phys. Rev. Lett. **64**, 1577 (1990); A. Sornette and D. Sornette, Tectonophysics **179**, 327 (1990); T. Chelidze and Y. Gueguen, Geophys. J. Int. **137**, 1 (1999); T. Chelidze, Y. Gueguen, and C. Ruffet, Geophys. J. Int. **137**, 16 (1999).